Marine Pollution Bulletin 223 (2026) 119020

Contents lists available at ScienceDirect

Marine Pollution Bulletin

journal homepage: www.elsevier.com/locate/marpolbul

# Assessing the risk of coastal oil strandings in the Brazilian equatorial margin: A numerical modeling approach

Francisco Flávio de Brito Borges [a,*], Pedro Paulo de Freitas [b], Wanessa Karoline Lima e Silva [a], Camilo Andrés Guerrero-Martin [a], Vando José Costa Gomes [a], Eduardo Siegle [c]

[a] *Faculty of Engineering, Federal University of Pará (UFPA), Salinópolis, Pará, Brazil*
[b] *Center for Marine Studies, Federal University of Paraná (UFPR), Pontal do Paraná, Brazil*
[c] *Oceanographic Institute, University of São Paulo (USP), São Paulo, Brazil*

ARTICLE INFO

*Keywords:*
Lagrangian modeling
Amazon shelf
North Brazil current
OpenDrift

ABSTRACT

The Brazilian Equatorial Margin (BEM) holds major ecological, climatic, and socio-economic importance and is emerging as a new frontier for offshore oil exploration in Brazil. This study aims to identify and characterize the preferential surface transport pathways of oil spills from four potential spill points located in the Potiguar (SPO), Barreirinhas (SBAR), Pará-Maranhão (SPAMA), and Foz do Amazonas (SFZA) basins. Lagrangian simulations were conducted with the OpenDrift model using surface velocity fields from the Surface Merged Ocean Current (SMOC) model. Validation confirms that SMOC accurately reproduces the spatio-temporal variability of surface currents, while OpenDrift proves reliable for simulating oil transport and dispersion. Results indicate that most of the BEM could be affected by potential spills, with preferential pathways and coastal stranding zones varying according to spill location. Spills from SPO and SBAR (points 1 and 2) show the highest impacts, with over 80 % intrusion on the continental shelf and more than 30 % coastal stranding, whereas SFZA (point 4) shows no intrusion or stranding. These pathways are modulated by trade wind variability and mesoscale activity of the North Brazil Current (NBC). Higher intrusion and stranding generally occur in summer and spring, though without a strong seasonal trend. The findings highlight the importance of identifying oil transport pathways to support region-specific contingency planning, as elevated stranding risks threaten sensitive coastal ecosystems and local livelihoods, underscoring the need to integrate operational oceanographic modeling into coastal management.

## 1. Introduction

Oil exploration and production activities pose significant environmental risks, particularly concerning chemical spills (Le Tan et al., 2023), which may result from shipping accidents, operational discharges, oil storage and handling, refining processes, and pipeline leakages (Abou Samra and Ali, 2024). The global increase in the use of crude oil and its derivatives makes the risk of oil pollution inevitable (Govindarajan et al., 2021), with approximately 90 % of industrial disasters occurring in marine environments (Galieriková and Materna, 2020). Once released into the marine environment, oil undergoes weathering processes such as evaporation, emulsification, and dissolution, which alter its physical-chemical properties and influence its persistence at sea (Abou Samra et al., 2021). The dispersion and transport of oil slicks are strongly influenced by oceanographic factors such as wind, waves, currents, sea surface temperature (SST), and bathymetry, whose spatial and temporal variability can modify spreading patterns and increase the risk of shoreline contamination (Abou Samra et al., 2021; Abou Samra and Ali, 2022, 2024).

The largest oil spill ever recorded off the coast of Brazil occurred between 2019 and 2020, affecting approximately 2890 km of coastline, including parts of the BEM (Soares et al., 2022; Pena et al., 2020). This event underscored the importance of understanding the physical processes governing mass exchange between the ocean and the continental shelf, including those oceanographic drivers that influence dispersion, to support oil spill response efforts (Zacharias et al., 2024). Oil spills pose severe threats to coastal ecosystems, economies, and communities, making their dispersion and stranding patterns critical for effective coastal management (Transportation Research Board and National Research Council, 2003). The fate of spilled oil, whether it disperses

* Corresponding author.
*E-mail address:* fl4vioborges@gmail.com (F.F.B. Borges).

https://doi.org/10.1016/j.marpolbul.2025.119020
Received 1 October 2025; Received in revised form 12 November 2025; Accepted 16 November 2025
Available online 19 November 2025

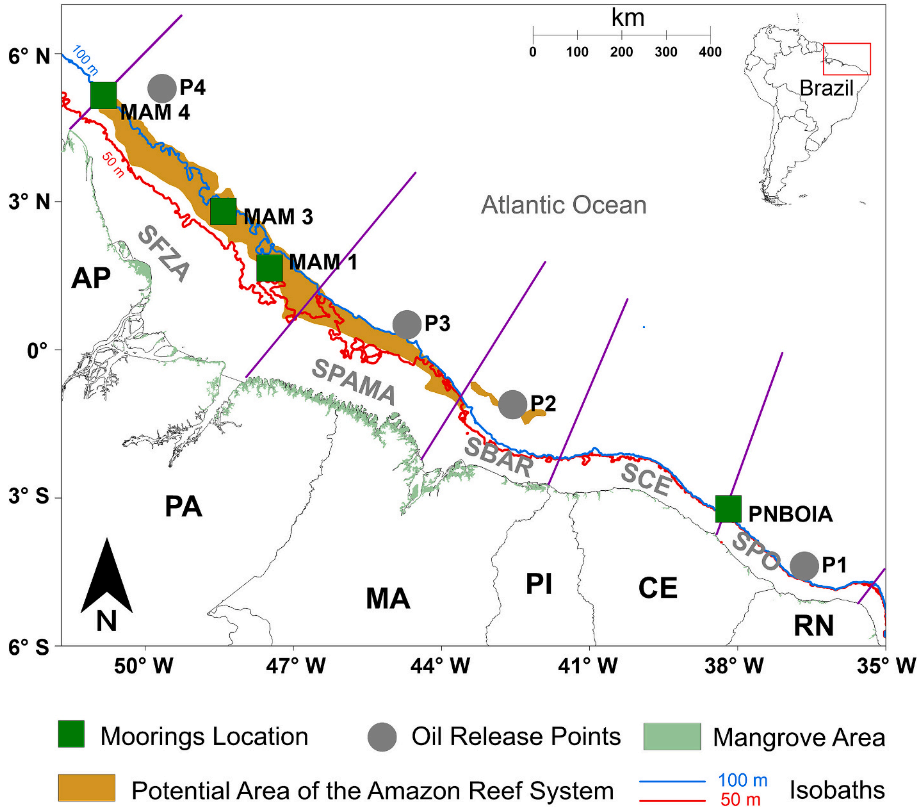


**Fig. 1.** Bathymetric Map of the Brazilian Equatorial Margin (BEM), covering the states of Amapá (AP), Pará (PA), Maranhão (MA), Piauí (PI), Ceará (CE), and Rio Grande do Norte (RN). Contour lines represent isobaths at 100 m (red) and 50 m (yellow). Magenta lines indicate sedimentary basin boundaries: Foz do Amazonas (SFZA), Pará-Maranhão (SPAMA), Barreirinhas (SBAR), Ceará (SCE), and Potiguar (SPO). Green square markers represent current measurements from the AMANDES project (MAM1, MAM3, and MAM4) and the PNBOIA project. Gray points (P1, P2, P3, and P4) indicate the locations of oil spills used in the Lagrangian model OpenOil/OpenDrift. The orange-shaded area represents the potential extent of the Amazon Reef System, while the green-shaded area corresponds to mangrove zones. The inset map shows the location of the study area. (For interpretation of the references to colour in this figure legend, the reader is referred to the web version of this article.)

offshore, accumulates on the continental shelf, or strands on coastlines, determines its ecological and socioeconomic impacts, affecting sensitive habitats such as mangroves, reefs, and fisheries (Peterson et al., 2003; Uno et al., 2017). Numerical modeling studies, such as those employing Lagrangian particle-tracking approaches, have become essential tools for predicting spill trajectories, identifying high-risk zones, and informing emergency response strategies (Reed et al., 1999; French-McCay, 2004).

The Brazilian Equatorial Margin (BEM), located between 52°W and 35°W and 7.5°N and 5.8°S, includes the sedimentary basins of Foz do Amazonas (SFZA), Pará-Maranhão (SPAMA), Barreirinhas (SBAR), Ceará (SCE), and Potiguar (SPO) (Fig. 1). The width of the equatorial continental shelf varies significantly, being narrower to the south of 3°S and widening northward near the Amazon River to about 100–300 km (Aguiar et al., 2022). Its hydrodynamics are driven by tides, trade winds, river discharge, and mesoscale activity from the North Brazil Current (de Freitas et al., 2025). It has great ecological, climatic, and socioeconomic importance (da Cruz et al., 2021; Louchard et al., 2021; Araújo et al., 2022) and represents a new frontier for offshore oil and gas exploration in Brazil (Milani et al., 2000; Mello et al., 2013; Ysaccis et al., 2023). The oil industry's interest in this region is driven by its geological characteristics, which are similar to those of successful exploration areas nearby, such as Guyana and Suriname (Hoorn et al., 2017; de Almeida et al., 2020), and reserves estimated at around 16 billion barrels (Ávila, 2022; Price and Mapes, 2023; Abelha, 2023). However, concerns regarding environmental impacts have led to restrictions imposed by the Brazilian Institute of Environment and Renewable Natural Resources (IBAMA) on oil exploration in the region, particularly due to its high biodiversity and the presence of sensitive ecosystems such as mangroves and mesophotic reefs (Zacharias et al., 2024; Mahiques et al., 2019; Moura et al., 2016).

The BEM is characterized by high-energy hydrodynamics driven by trade winds, waves, tides, river discharge, and the North Brazil Current (NBC), all of which play an important role in driving mass fluxes between the ocean and the continental shelf (Prestes et al., 2018; Aguiar et al., 2022; de Freitas et al., 2025).The seasonal migration of the Intertropical Convergence Zone (ITCZ) results in changes in the prevailing trade wind direction in the region, with northeast trade winds dominating during the austral summer and southeast trade winds prevailing during the austral winter (de Freitas et al., 2025; Lessa et al., 2021). The tidal regime is predominantly semidiurnal (M2), with tidal ranges exceeding 4 m across the shelf; values reach ~6 m near Cabo Norte (western shelf) and can exceed 8 m in São Marcos Bay (eastern shelf) (de Freitas et al., 2025; Aguiar et al., 2022). Significant wave heights in the region are modulated by the trade wind regime, with prevailing directions from east to northeast, reflecting the strong wind forcing that dominates the Equatorial Brazilian Margin (Aguiar et al., 2022). River discharge is strongly seasonal; the Amazon River reaches maximum values around $2.0 \times 10^5$ $m^3$ $s^{-1}$ during the austral summer (Prestes et al., 2018; de Freitas et al., 2025), with peak flows typically in May–June and minima in October–November (Prestes et al., 2018).

Lessa et al. (2021) used global numerical model results and observational data to investigate oil transport along the Brazilian coast in 2019. Their results suggest that the NBC and shelf currents driven by trade winds play a critical role in advecting oil along the BEM. Nobre et al. (2022) performed simulations of particle tracking and oil

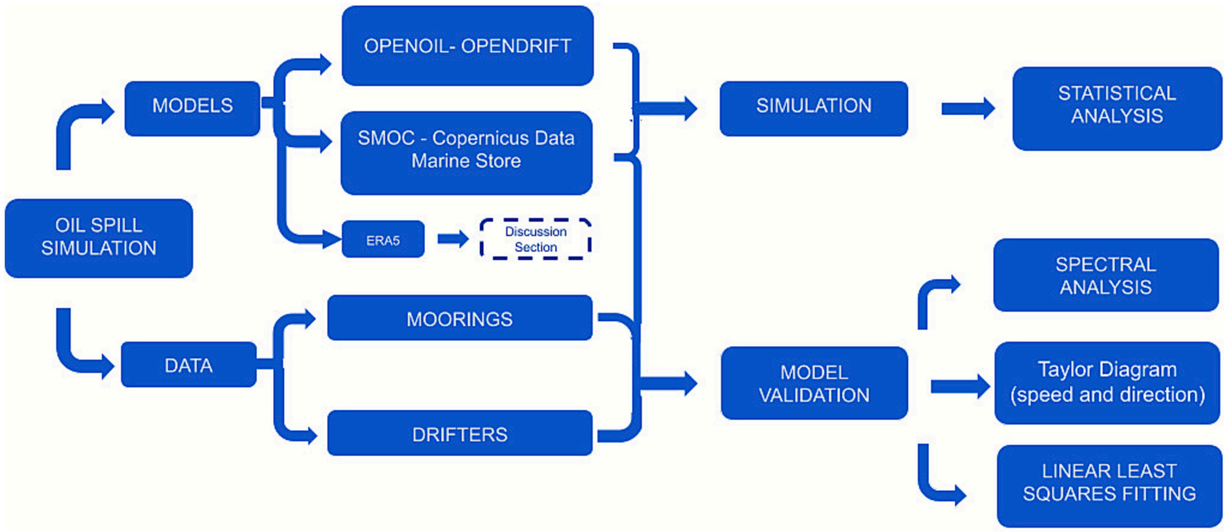


**Fig. 2.** Flowchart of the methodology applied in this study, summarizing the main steps of data preparation, oil spill simulation, model validation, and analysis.

dispersion along the northwest coast of Brazil and highlighted the significant role of the South Equatorial Current (SEC) in transporting the oil below the surface. In addition, Calzada et al. (2021), using the PETROMAR-3D Lagrangian model, showed that oil spilled in offshore regions north of 6°S has a higher probability of reaching the northeastern Brazilian coast between January and October.

Despite significant scientific advances in understanding the physical mechanisms of oil dispersion along the BEM, knowledge gaps remain regarding: (i) the variability in preferred pathways for oil intrusion from the oceanic region to the continental shelf depending on the release point, and (ii) the temporal variability of oil intrusion and its impact on coastal areas. Therefore, using velocity measurements from four moorings, velocity and trajectory data from drifters, and three years of Lagrangian simulations, this study aims to characterize oil spill patterns along the BEM from four spill points. This involves: (i) identifying preferential intrusion pathways from the oceanic region to the continental shelf based on four virtual spills in the exploratory basins of Potiguar (SPO), Barreirinhas (SBAR), Pará-Maranhão (SPAMA) and Foz do Amazonas (SFZA); (ii) characterizing the spatial and temporal variability of oil intrusion into the shelf during different seasons (summer/autumn and winter/spring); and (iii) analyzing the spatial and temporal variability of oil reaching the coastline, depending on the spill location and seasonal conditions.

## 2. Methodology

Oil dispersion was simulated using the OpenDrift OpenOil model, forced by Surface Merged Ocean Current (SMOC) model fields that include currents, waves, and tides. The simulation was validated using direct current observations and statistical analyses, including linear least squares fitting, skill metrics, and a Taylor diagram to assess agreement between modeled and observed current speed and direction. Fig. 2 summarizes the methodology, outlining the steps involved in data preparation, simulation execution, result validation, and analysis.

### *2.1. In situ data*

#### *2.1.1. Moorings data*

In this study, hourly velocity measurements from three moorings of the AMANDES project (Le Bars et al., 2010; Prestes et al., 2018; de Freitas et al., 2025), collected between April and July 2008, and from one buoy of the PNBOIA program (https://www.marinha.mil.br/chm/dados-do-goos-brasil/pnboia-mapa), obtained in December 2016 and April 2017, were used to validate the velocity field of the numerical model results.

The AMANDES moorings (MAM1, MAM3, MAM4) were deployed on the Amazon Continental Shelf between April and July 2008. They operated with instruments positioned at fixed depths within the upper

**Table 1**
Characterization of velocity measurements from the moorings of the AMANDES project and the buoy of the PNBOIA along the Brazilian Equatorial Margin (BEM).

| Period analyzed | |
|---|---|
| Start date | End date |
| Dec 1st, 2016 | Apr 15th, 2017 |
| Apr 12th, 2008 | Jul 16th, 2008 |
| Apr 13th, 2008 | Jul 15th, 2008 |
| Apr 17th, 2008 | Jul 11th, 2008 |

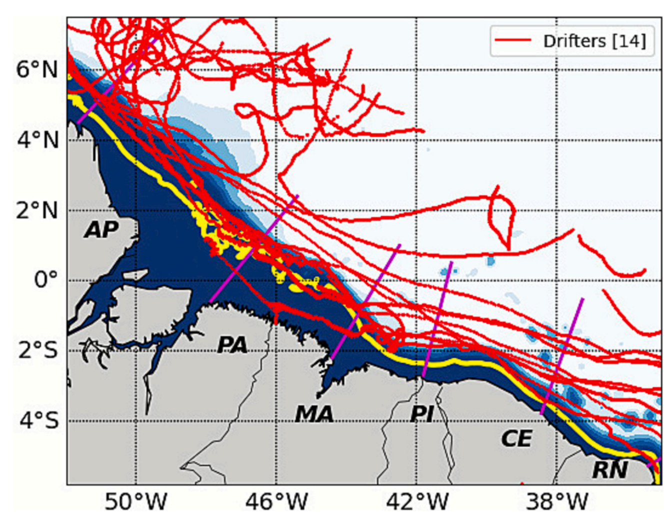


**Fig. 3.** Trajectories of the drifters (red lines) in the BEM between 2021 and 2023. Contour lines represent isobaths at 50 m (yellow). Magenta lines indicate the boundaries of sedimentary basins: Foz do Amazonas (SFZA), Pará-Maranhão (SPAMA), Barreirinhas (SBAR), Ceará (SCE), and Potiguar (SPO). AP, PA, MA, PI, and CE represent the Brazilian states of Amapá, Pará, Maranhão, Piauí, and Ceará, respectively. (For interpretation of the references to colour in this figure legend, the reader is referred to the web version of this article.)

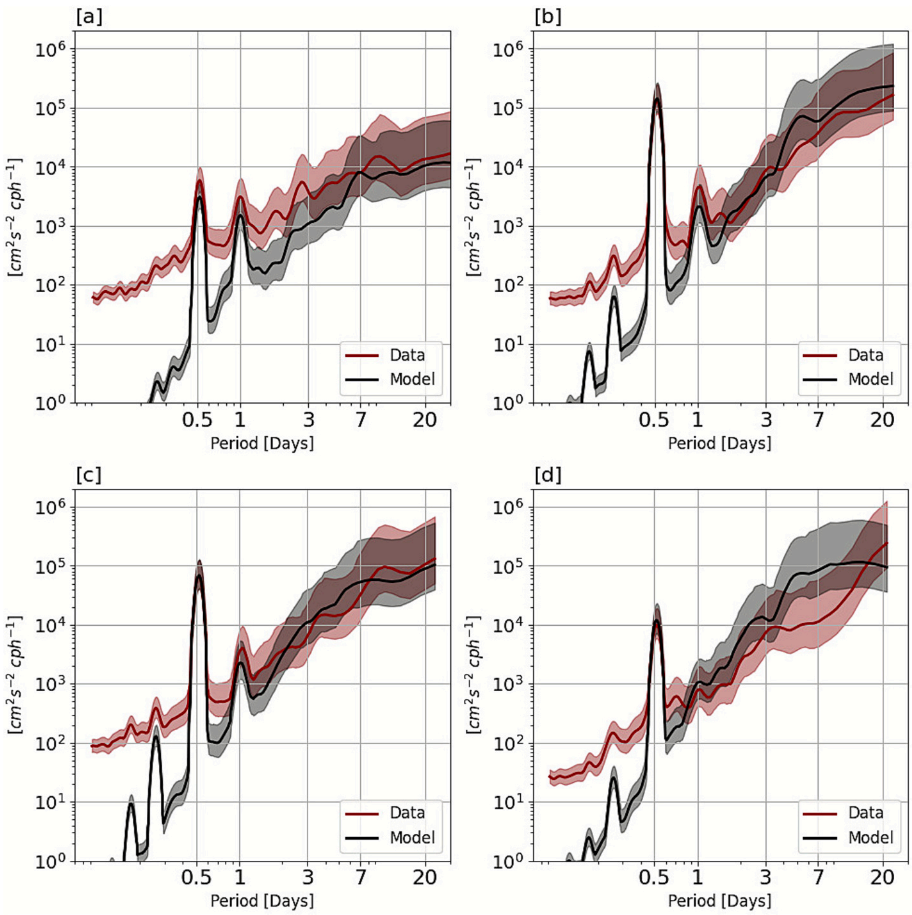


**Fig. 4.** Rotary spectral analysis of the raw surface velocity components U and V from the moorings PNBOIA [a], MAM1 [b], MAM3 [c], and MAM4 [d] (in red), and the SMOC model (in black), at the same location. The shaded area represents the 99 % statistical confidence limit. The geographical locations of the stations and their respective periods are shown in Fig. 1 and Table 1. (For interpretation of the references to colour in this figure legend, the reader is referred to the web version of this article.)

water column. Each mooring was equipped with a Nortek Aquadopp ADCP (1200 kHz) at shallower depth and an Aanderaa RCM7 current meter at deeper depth, both including temperature and conductivity sensors (de Freitas et al., 2025). These instruments provided velocity, temperature, and salinity time series, resolving tidal variability (Prestes et al., 2018).

The buoy considered corresponds to the Metocean Fortaleza buoy, moored at 200 m depth off Fortaleza. Built by AXYS (model AXYS-3 M, 3.4 m diameter, 1500 kg), the buoy was equipped with two anemometers (3.47 m and 4.0 m height), meteorological sensors and oceanographic sensors. An ADCP with 3.5 m vertical bins, starting at 0.5 m depth, provided current profiles throughout the entire water column. This configuration enabled the monitoring of both surface and subsurface currents, as well as wave parameters. Tidal variability was indirectly captured from the ADCP current time series.

The location, measurement depths, and observation periods are summarized in Table 1 and illustrated in Fig. 1.

#### 2.1.2. *Drifters*

Fourteen drifters with trajectories and velocity measurements within the Brazilian Equatorial Margin (BEM) between January 2021 and December 2023 (Fig. 3) were selected from the Coriolis platform (https://dataselection.coriolis.eu.org/) to validate the surface velocity field of the numerical model results.

### 2.2. *Numerical modeling*

#### 2.2.1. *Surface merged ocean current (SMOC)*

In this study, hourly surface velocity fields from the Surface Merged Ocean Current (SMOC) model, covering the period from January 1, 2021, to December 31, 2023, were used to force lagrangian simulations of oil spills along the Brazilian Equatorial Margin (BEM) (Fig. 1). The SMOC model outputs are available through the Copernicus Marine Environment Monitoring Service (CMEMS) (https://data.marine.copernicus.eu/product/GLOBAL_ANALYSISFORECAST_PHY_001_024/description). The SMOC model presents a horizontal resolution of 1/12° and incorporates wave and tidal drift in its velocity fields. The domain used in this study spans approximately 240 grid points in the x-direction and 160 in the y-direction. Its hourly temporal resolution, combined with the inclusion of tidal effects, makes the SMOC model particularly suitable for realistic numerical studies of the processes governing oil dispersion along the Brazilian Equatorial Margin (BEM).

#### 2.2.2. *Lagrangian modeling*

Lagrangian modeling was performed to identify preferential pathways for surface oil intrusion into the BEM and to investigate how the spatiotemporal variability of the NBC modulates these intrusions. For this purpose, we used the OpenOil module of the Opendrift model (https://opendrift.github.io/), which is specifically designed for petroleum drift modeling (Dagestad et al., 2018; Pavlov et al., 2023; Nguyen et al., 2024). The model domain encompasses the entire Brazilian equatorial margin, extending from 6.0°S to 10.0°N and from 52.0°W to

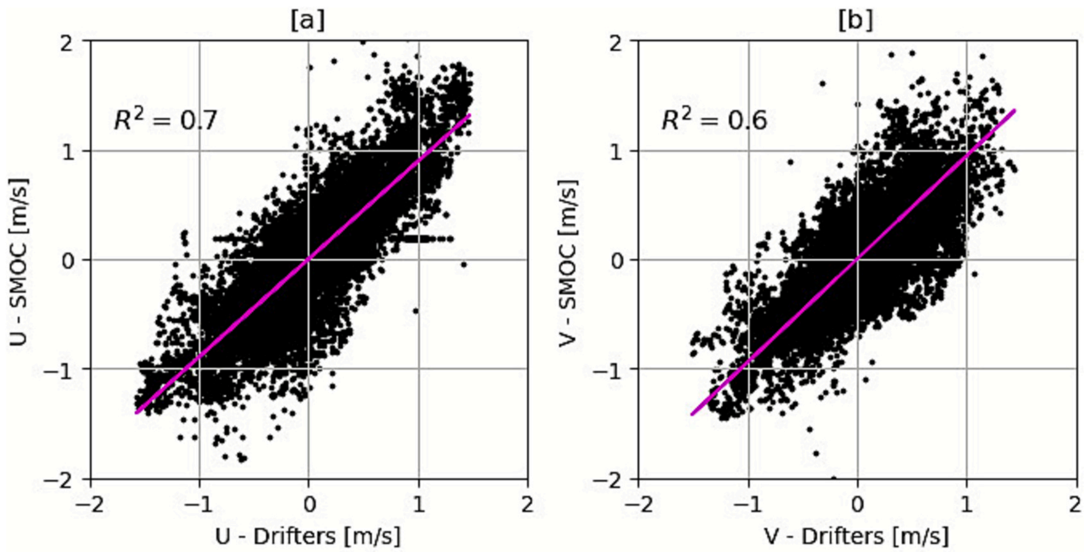


**Fig. 5.** Scatter plots comparing surface velocity measurements from drifters and the SMOC model for the *u* [a] and *v* [b] velocity components. This analysis is based on measurements from 14 drifters that crossed the BEM between 2021 and 2024. The magenta line in each panel represents the least-squares fit between the observed and modeled velocity series. The $r^2$ value indicates the coefficient of determination. The geographical locations of the drifter measurements are shown in Fig. 2. (For interpretation of the references to colour in this figure legend, the reader is referred to the web version of this article.)

30.0°W (Fig. 1), highlighted by the red line inset), with the same horizontal resolution used in the SMOC model.

The Lagrangian experiments were carried out over a three-year period, from 2021 to 2023, involving hourly oil releases at four specific locations within the producing basins of the BEM (Fig. 1), and a total of 26,280 oil particles were released at each point. Particle advection was computed using a one-hour time step with the fourth-order Runge-Kutta (RK4) method, excluding horizontal diffusion. It is important to note that the simulations did not account for oil weathering processes (e.g., evaporation, emulsification, dissolution) or environmental drivers such as sea surface temperature and bathymetry. The OpenDrift–OpenOil setup used here represents only the surface advection of oil particles as driven by SMOC velocity fields, allowing the analysis to focus on circulation-driven dispersion patterns, with emphasis on preferential intrusion pathways and coastal stranding. Each trajectory was individually tracked to identify intrusion events and to determine their specific locations and periods of occurrence. The oil type used in this study was “BAHIA,” sourced from the ADIOS oil database (ADIOS/NOAA) (https://adios.orr.noaa.gov/oils/AD00102). This oil has a density of 0.848 g/cm$^3$ and an API gravity of 35.2, classifying it as a light oil (Pabón and de Souza Filho, 2019). The selection of this oil type is based on studies conducted by Hoorn et al. (2017) and de Almeida et al. (2020). These studies provide seismic mapping results for the southern region of the Foz do Amazonas Basin and the entirety of the Pará-Maranhão Basin, indicating a strong likelihood of such light oil deposits in the area.

### 2.3. ERA5 data

This study utilized the u and v wind velocity components from ERA5 (https://cds.climate.copernicus.eu/datasets/reanalysis-era5-single-levels?tab=download) from 2021 to 2023 to support the analysis and discussion of oil dispersion processes along the Brazilian Equatorial Margin.

### 2.4. Analysis

To quantify the accuracy and reliability of the SMOC velocity field, a comparison of drifter velocity measurements and model results was performed using rotary spectral analysis and correlation by linear regression. Based on previous studies on the morphology of the continental shelf on BEM (Nittrouer and DeMaster, 1986; Lavagnino et al., 2020; Landim Dominguez et al., 2023), this study used the detection of oil at the 50 m isobath with a minimum duration of one day as the criterion for intrusion into the continental shelf. A particle was considered to have intruded when it remained within this isobath for at least 24 consecutive hours, regardless of the number of particles involved. The percentage of intrusion on the continental shelf was calculated based on the total number of oil particles released, while the percentage of oil stranded on the coast was quantified based on the total amount of oil intruded on the shelf. When a particle reaches the domain boundary (Fig. 1), its simulation is terminated and it is not included in the calculation of coastal intrusion or stranding.

When a particle reaches the domain boundary (Fig. 1), its simulation is terminated, and the particle is treated as missing data. It is excluded from the calculation of coastal intrusion or stranding only if it does not meet either criterion. Particles that satisfy the shelf intrusion condition (presence within the 50 m isobath for at least 24 consecutive hours) or that strand along the coast are retained in the analysis. While oil viscosity is known to influence horizontal dispersion, this study used a single light oil type (BAHIA, API 35.2). Therefore, the intrusion percentages reported here reflect the behavior of this specific oil under the given forcing conditions, without addressing variability associated with different oil types or viscosities.

## 3. Results

This section is divided into two parts: (i) validation of the SMOC model and (ii) characterization of the spatiotemporal variability of oil intrusion into the BEM.

### 3.1. SMOC model validation

Fig. 4 shows the rotary spectral analysis of the raw velocity time series from the AMANDES and PNBOIA moorings (see Section 2.1.1), as well as from the SMOC model, at the same location. Although the velocity data cover different periods (Table 1) than those simulated by the SMOC model, the energy levels in the frequency domain are similar within the statistical confidence limits (shaded area), suggesting that the SMOC model effectively captures the temporal variability of currents in

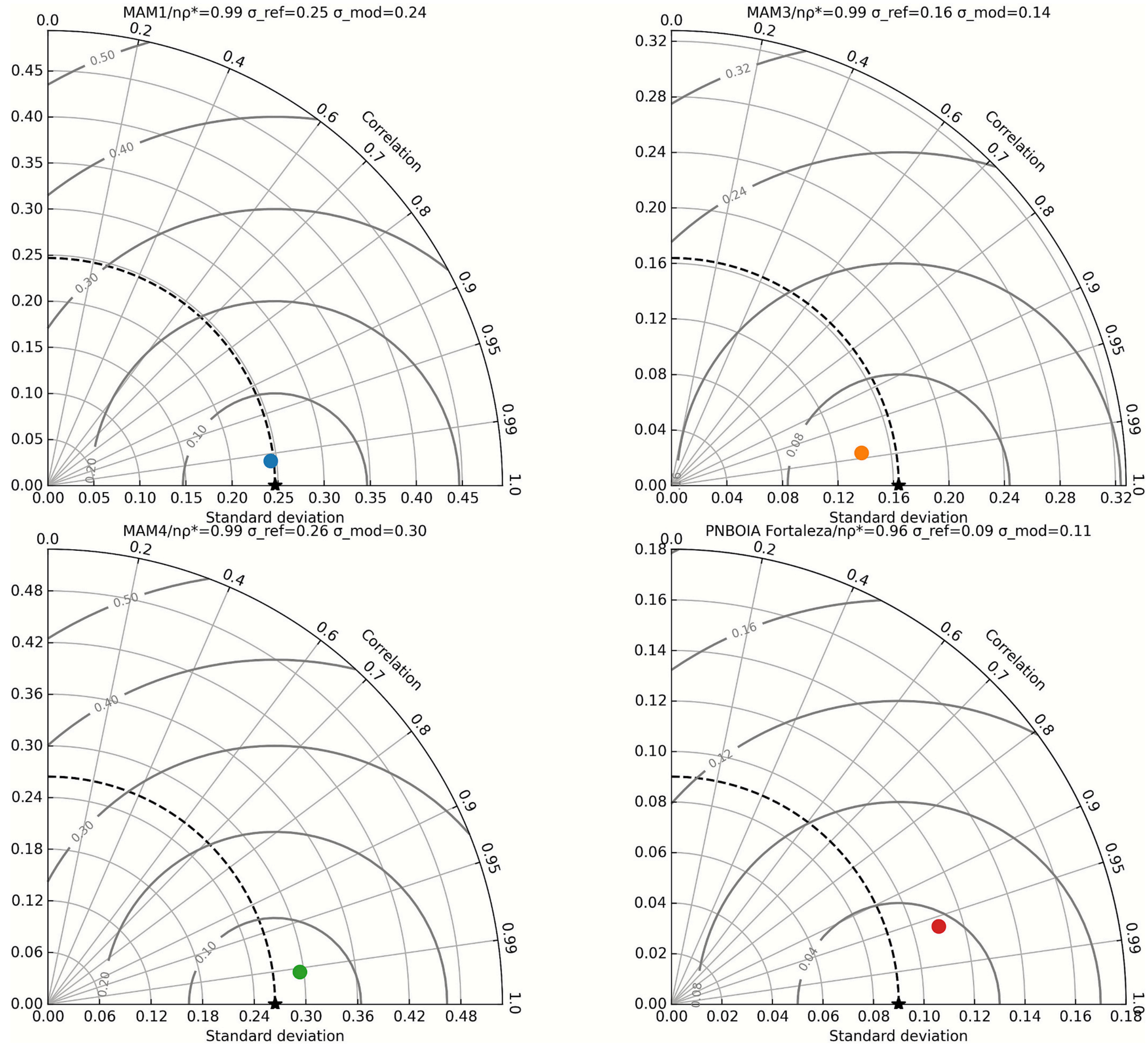


**Fig. 6.** Taylor diagrams comparing the SMOC model (2021−2023) and observational current data at MAM1 [a], MAM3 [b], MAM4 [c], and PNBOIA Fortaleza [d]. The results show very high correlations (ρ ≈ 0.96–0.99) and similar standard deviations between model and observations, indicating that the SMOC model reproduces both the correlation and the same level of variability at each site.

the BEM associated with semidiurnal (0.5 days) and diurnal (1 day) tidal periods, as well as low-frequency variations for periods longer than 3 days. This spectral comparison between modeled and observed currents served as the primary verification method to assess the SMOC model's capability in reproducing the dominant temporal variability of currents in the region.

Based on the velocity measurements of 14 drifters that crossed the BEM between 2021 and 2024, the accuracy of the SMOC model was assessed using a least-squares fit for each velocity component, as shown in Fig. 5 [a, b]. The scatter plots show good agreement between the observations and the model, with coefficients of determination ($r^2$) of 0.7 and 0.6 for the u and v velocity components, respectively. This complementary validation approach reinforces the reliability of the SMOC model in representing surface current variability across the BEM.

Fig. 6 presents Taylor diagrams comparing modeled and observed currents at the same mooring locations. The results show very high correlations (ρ ≈ 0.96–0.99) and, importantly, that the model and the observations present nearly identical standard deviations. This indicates that, at each measurement site, the SMOC model not only correlates strongly with the observed currents but also reproduces the same level of variability, which is a key aspect of model validation.

Together, the spectral analysis, the regression with drifter data, and the Taylor diagrams provide consistent evidence that the SMOC model adequately reproduces both the temporal structure and the magnitude of surface currents in the BEM.

### 3.2. *Spatiotemporal variability of oil intrusion into the BEM*

The three-year surface oil spill simulation at different BEM points (Fig. 1) revealed spatial variations in oil intrusion onto the continental shelf and coastal stranding depending on the oil release location (Fig. 7). The oil release points at SPO (point 1) and SBAR (point 2) had the

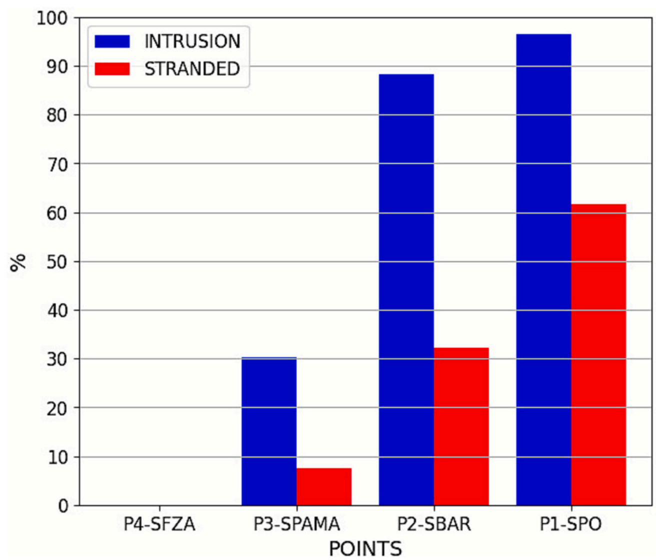


**Fig. 7.** Histogram showing the percentage of oil intrusions onto the continental shelf (blue) and coastal strandings (red) along the BEM from releases of 26.280 oil particles at Points P1 (SPO), P2 (SBAR), P3 (SPAMA), and P4 (SFZA). The percentage of intrusion on the continental shelf was calculated based on the total number of oil particles released, while the percentage of oil stranded on the coast was quantified based on the total amount of oil intruded on the shelf. The geographical locations of Points P1, P2, P3, and P4 are shown in Fig. 1. (For interpretation of the references to colour in this figure legend, the reader is referred to the web version of this article.)

highest occurrence of intrusion onto the continental shelf, accounting for 96 % and 88 % of the total particles, respectively, and 61 % and 32 % of the intruded particles for coastal stranding. At SPAMA (Point 3), the released oil exhibited lower intrusion and stranding compared to the eastern BEM points, accounting for 31 % and 7 % of the total particles, respectively. The oil release simulation at SFZA (point P4), on the other hand, shows no occurrence of intrusion or stranding along the entire BEM.

The locations of oil intrusion into the continental shelf and coastal stranding for each release point are shown in Fig. 8. The results from the releases at SPO (Point 1) (Fig. 8[a]) indicate that oil intrusions occur predominantly on the adjacent Potiguar continental shelf (28 %) and in the SCE sector (42 %), while coastal strandings reach their maximum in the SBAR sector (36 %), located on the Maranhão continental shelf. The oil released at SBAR (Point 2) (Fig. 8[b]) follows a preferential intrusion pathway toward the Maranhão and Pará shelves (77 %), which are part of the SPAMA sector, with maximum stranding (32 %) occurring along the coast of the SFZA sector. The dispersion of oil particles released at SPAMA (point 3) (Fig. 8[c]) follows the same pattern observed at the other points, with intrusions and strandings occurring on the adjacent continental shelf and coast. In this case, the highest values are observed in the SFZA sector, reaching 19 % for intrusions and 26 % for strandings. In contrast, no intrusions or strandings are observed for releases in the SFZA sector (point 4) (Fig. 8[d]).

The seasonal variability of oil intrusion into the continental shelf from releases at BEM (Points 1–4) is presented in Fig. 9. For releases in the SPO sector (Point 1) (Fig. 9[a]), more intrusion events are observed during summer and spring in the SPO (9 % in both seasons) and SCE (9 % in both seasons) shelves. In addition, a clear seasonal pattern of intrusion is evident in the SBAR and SPAMA shelves, with higher occurrences in autumn (5 %) and winter (7 %) for SBAR and exclusively in winter (3 %) for SPAMA. For releases from SBAR (Point 2) (Fig. 9[b]), oil intrusion affects the SPAMA shelf more during spring (23 %) and summer (19 %). However, the small percentage differences compared to autumn and winter (both 17 %) hinder the identification of a clear seasonal pattern. In contrast, for releases in the SPAMA sector (Point 3) (Fig. 9[c]), most intrusions into the SFZA continental shelf occur predominantly during the austral summer (11 %).

The quantification of oil stranded on the coast during each season is shown in Fig. 10. For releases in the SPO sector (Point 1) (Fig. 10[a]), oil stranding on the coast occurs most frequently in summer (10 %) and spring (8 %) in SCE; spring (13 %), winter (11 %), and summer (10 %) in SBAR; winter (5 %) and autumn (4 %) in SPAMA; and winter (4 %) in SFZA. For oil released in the SBAR sector (Point 2) (Fig. 10[b]), the highest stranding occurred during spring (15 %) in SFZA coast, which coincides with the period of maximum intrusion into the continental shelf (Fig. 9[b]).

For releases from the SPAMA sector (point 3)(Fig. 10[c]), most of the oil stranded occurred during the summer (24 %) in SFZA coast, the same period observed for oil intrusion into the continental shelf. For releases from the SFZA sector (Point 4) (Fig. 10[d]), no coastal stranding was observed along the sectors defined in this study). However, this does not imply that oil released in this region does not reach any coastline. Instead, it suggests that the modeled oil drift may be transported outside the Brazilian coast defined in the study domain (Fig. 1), potentially affecting other regions further west or even reaching neighboring countries or of the Caribbean. Although these areas were outside the spatial boundaries analyzed in this work, such westward drift possibilities should be acknowledged, as they emphasize the need for a broader regional oil spill risk assessment beyond national borders.

## 4. Discussion

Validation of the Lagrangian modeling used in this study was challenging due to the limited availability of current data in the BEM. Based on comparative analysis using freely available surface velocity measurements, the SMOC model adequately simulates the spatio-temporal variability of currents in the region, supporting the results obtained from Lagrangian simulations using the OpenDrift model (OpenOil module).

The quantification of oil intrusion and stranding along the BEM indicates that the entire region could be affected by a potential spill. However, the origin of the spill plays a critical role in determining the extent and specific areas affected. These results show that the percentage of oil intrusion into the continental shelf and of stranding along the coastline indicate that oil spills in the producing basins east of the BEM (SPO and SBAR) pose a serious challenge to the entire northern Brazilian continental shelf and coastline (Fig. 7). In contrast, basins located west of the BEM may have very low intrusion rates or even no intrusion, as observed in the SFZA oil spill experiments. The percentage reduction in oil intrusion and stranding from the SPAMA producing basin (point 3), and the absence of intrusion and stranding from SFZA (point 4) can largely be explained by a combination of factors that prevent oil intrusion onto the continental shelf. These factors include: (i) the absence of significant variation in the orientation of the continental shelf break isobaths beyond the SPAMA basin, and (ii) the considerable width of the Amazon continental shelf.

Our results also indicate that the most sensitive coastal habitats, including mangroves and beaches, are disproportionately affected by oil stranded from specific spill locations. The highest stranding percentages occur during the austral summer and spring, particularly from release point 2 (SBAR basin), where up to 24 % of released particles reached the coastline. In these scenarios, the northern and northeastern portions of the BEM, home to extensive mangrove ecosystems, are most exposed to oil contamination. The spatial overlap between stranding zones and ecologically sensitive areas underscores the critical need for targeted protection and response plans.

The pattern of oil intrusion and stranding along the coast (Fig. 8) confirms the modulating effect of wind-driven surface circulation as the primary mechanism of oil dispersion in the BEM. Fig. 11 shows the seasonal surface circulation on the BEM, highlighting the temporal

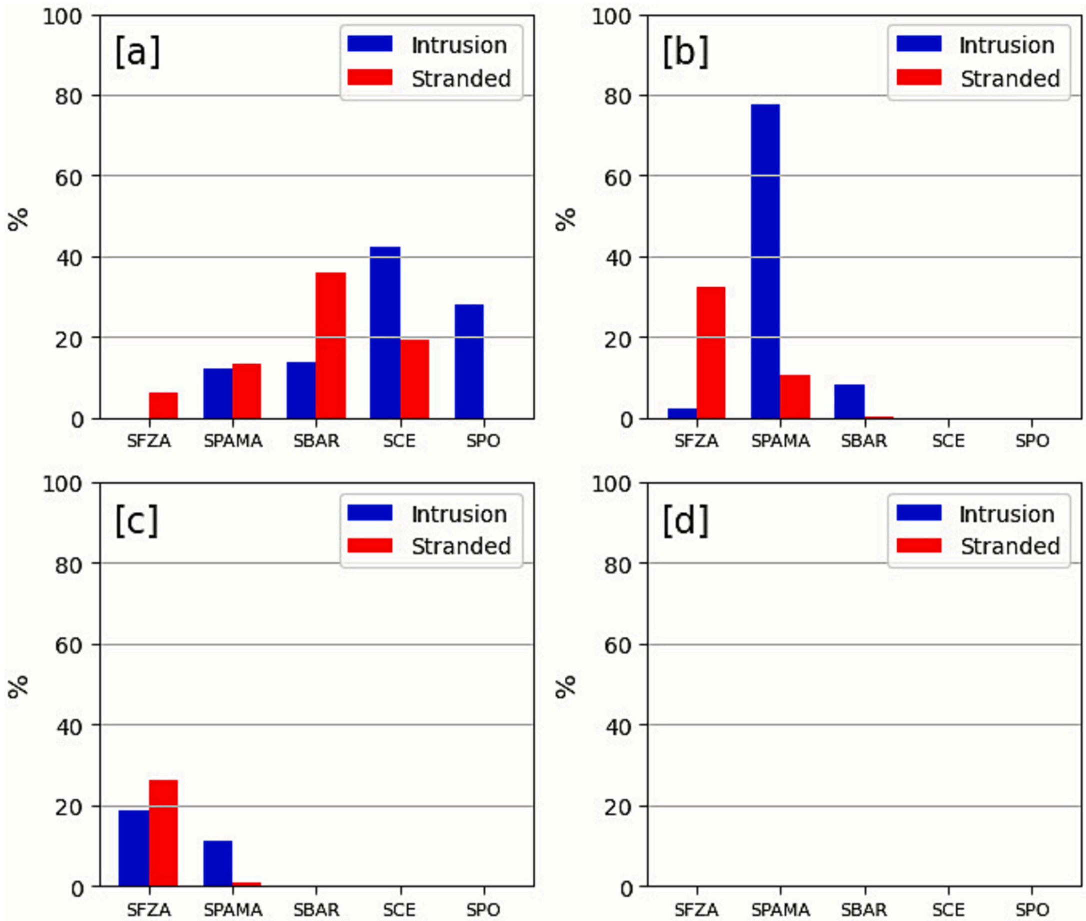


**Fig. 8.** Histograms showing the percentage of released oil particles that intrude into the continental shelf (blue) and those that stranded in the coastal region (red), quantified by sectors (SFZA, SPAMA, SBAR, SCE, and SPO) along the BEM. Panels [a–d] correspond to the results from release of 26.280 oil particles at points P1, P2, P3, and P4, respectively. The percentage of intrusion on the continental shelf was calculated based on the total number of oil particles released, while the percentage of oil stranded on the coast was quantified based on the total amount of oil intruded on the shelf.The geographical locations of points P1, P2, P3, and P4 are shown in Fig. 1. (For interpretation of the references to colour in this figure legend, the reader is referred to the web version of this article.)

variability of the NBC. During the austral summer and fall (Fig. 11[a,b]), the current shows an average flow parallel to the continental shelf, similar to a jet. In contrast, during winter and spring (Fig. 11[c,d]), the NBC retroflects from 5°N. Fig. 12 shows the average wind circulation on the BEM during the austral summer, autumn, winter and spring. The seasonality of the ITCZ modulates the intensity and prevailing direction of the trade winds, with NNE winds prevailing in summer and fall and SSE winds in winter and spring (Nittrouer and DeMaster, 1996).

The seasonal variability in oil intrusion patterns across different producing basins (Fig. 9) highlights the complexity of the factors regulating ocean-shelf exchange in the BEM region. Summer and spring are, in most scenarios (Fig. 9[a,b,c]), the periods with the highest percentage of oil intrusion on the shelf due to the combination of: i) the average NBC circulation in the form of a jet adjacent to the shelf break, and ii) trade winds blowing perpendicular to the orientation of the isobaths. In addition, the mesoscale activities of the NBC were identified by Zacharias et al. (2024) as critical to understanding oil dispersion patterns along the BEM. These results corroborate with previous studies about Amazon hydrodynamics and ocean-continental shelf exchanges in the region (Lessa et al., 2021; Aguiar et al., 2022; Goes et al., 2023; de Freitas et al., 2024).

The entire coast along the BEM, except for the SPO (Fig. 10), showed oil stranding. During summer and spring, the northeast winds increase intrusions and oil stranding at the coast (Fig. 11), in agreement with the seasonal patterns of wind-driven surface circulation described by Lessa et al. (2021) and Aguiar et al. (2022). Although the average surface wind-driven circulation on the continental shelf modulates a stronger along-shelf transport of oil, chances of oil stranding reach values of up to 24 % in SFZA sector. The BEM hosts a variety of coastal environments, including beaches, estuaries, reefs and extensive mangrove areas. The dispersion and strandings of oil spills have high impacts on such environments. For example, oil stranding on beaches smothers intertidal organisms (e.g., crabs, mollusks, polychaetes, etc. (e.g. Ozorio et al., 2024), reduces sediment permeability, and persists for years due to slow degradation in anoxic layers (e.g. Hayworth et al., 2011). Beaches may bury oil temporarily, but re-exposure during high-energy events perpetuates ecological damage (Huettel, 2022). In mangroves, oil coats pneumatophores and prop roots, impairing gas exchange and causing tree mortality within a few weeks to months (Duke et al., 1997). The complex root structure traps oil, leading to chronic contamination that disrupts nursery habitats for fish and crustaceans (Lewis et al., 2011; Nunes et al., 2023). Mangroves' low recovery rates (decades to centuries) exacerbate socio economic losses for coastal communities reliant on fisheries (Duke, 2016; Santos et al., 2012). Therefore, our results highlight the urgent need for region-specific oil spill contingency plans. High stranding risks threaten sensitive coastal ecosystems and livelihoods, underscoring the importance of integrating oceanographic modeling into proactive coastal zone management strategies.

## 5. Conclusion

This study contributes to quantifying the spatiotemporal variability

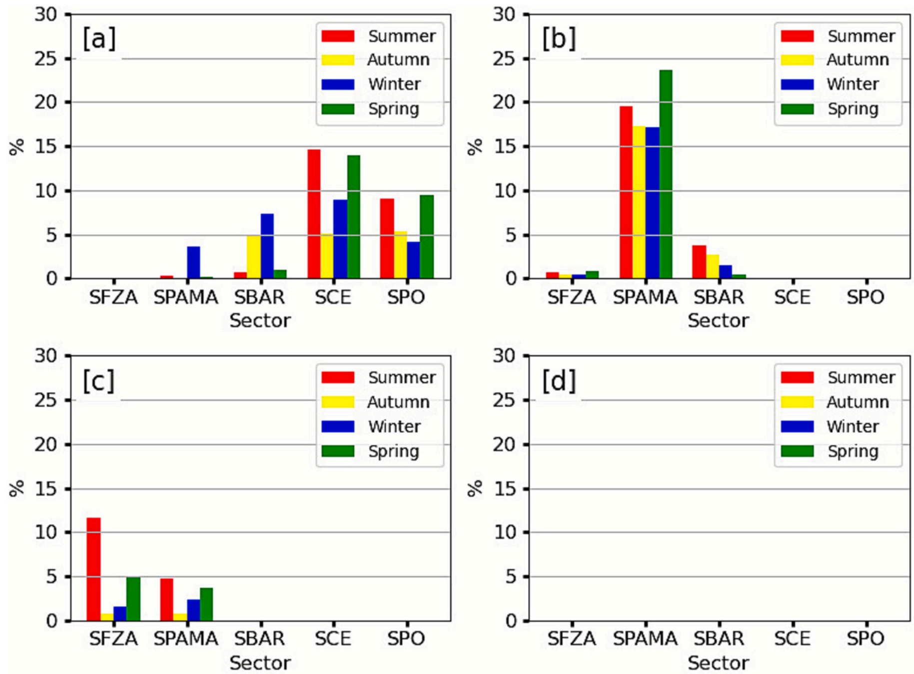


**Fig. 9.** Characterization of oil intrusion into the continental shelf across the BEM sectors during the austral summer (red), autumn (yellow), winter (blue), and spring (green). Panels [a–d] illustrate the seasonal variation of intrusions corresponding to different release point configurations: P1, P2, P3, and P4, respectively. The percentage of intrusion on the continental shelf was calculated based on the total number of oil particles released. The geographical locations of these points are shown in Fig. 1. (For interpretation of the references to colour in this figure legend, the reader is referred to the web version of this article.)

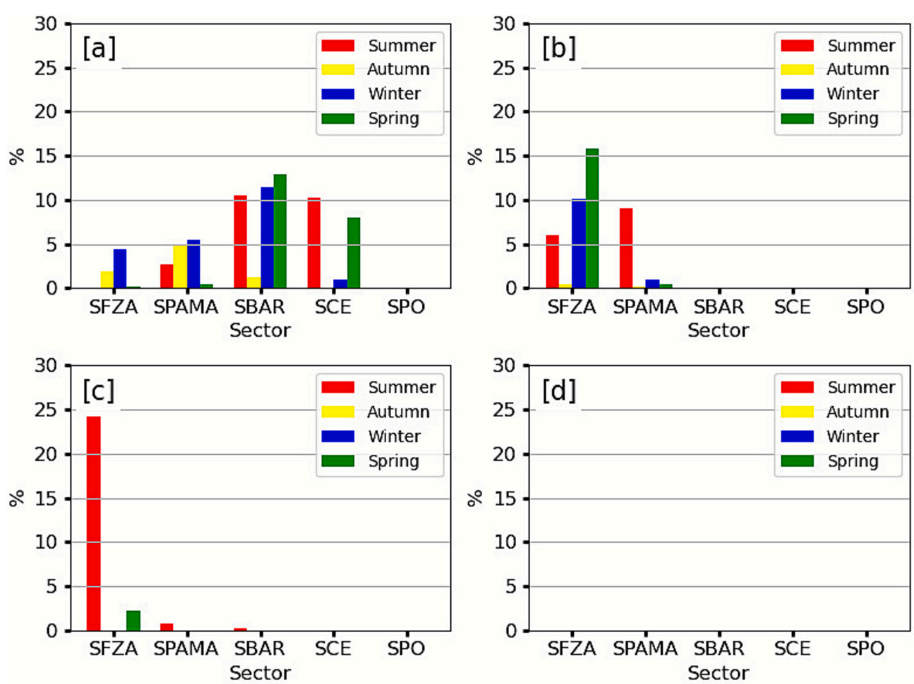


**Fig. 10.** Characterization of oil stranded on the coast along the BEM sectors during the austral summer (red), autumn (yellow), winter (blue), and spring (green). Panels [a–d] illustrate the seasonal variation of stranding corresponding to different release point configurations: P1, P2, P3, and P4, respectively. The percentage of oil stranded on the coast was quantified based on the total amount of oil that intruded on the shelf. The geographical locations of these points are shown in Fig. 1. (For interpretation of the references to colour in this figure legend, the reader is referred to the web version of this article.)

of ocean-shelf exchange processes in the context of oil spill simulations in the BEM. The findings enhance the assessment of potential risks associated with exploration activities in the region and help identify coastal areas most vulnerable to offshore oil spill impacts. The analysis confirms that the SMOC model accurately represents the spatiotemporal variability of surface currents in the BEM, while the OpenDrift model proves to be a valuable tool for oil spill investigations, providing results consistent with previous studies in the area, such as those reported by Lessa et al. (2021), Aguiar et al. (2022), Goes et al. (2023), and de Freitas et al. (2024).

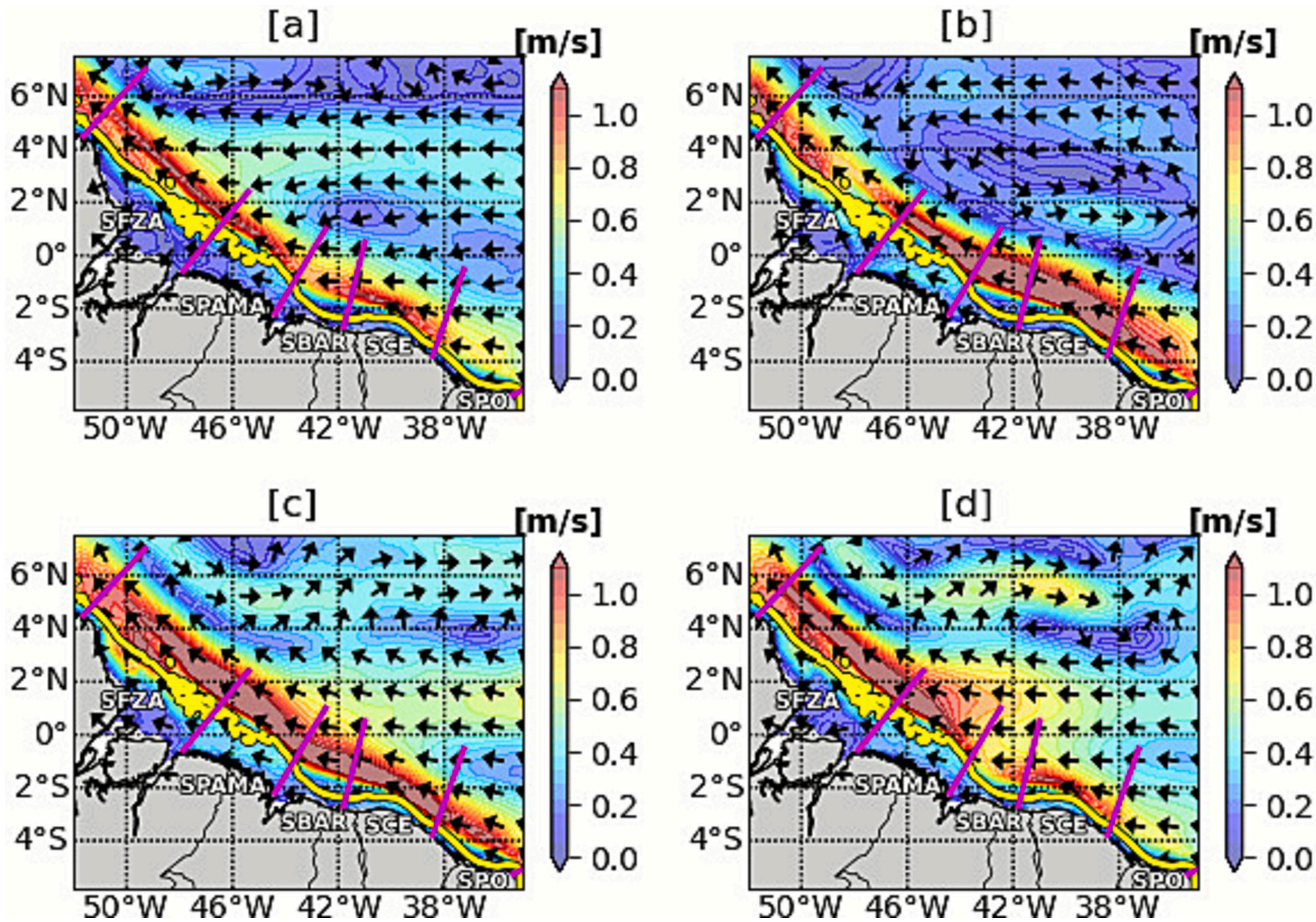


**Fig. 11.** Surface currents along the BEM based on three years (2021–2023) of SMOC model simulations. Panels [a-d] show the mean seasonal circulation for the austral summer, autumn, winter, and spring, respectively. The 50 m isobath (yellow line) marks the approximate mid-shelf region, while the magenta lines mark the boundaries of the exploratory basins as shown in Fig. 1. (For interpretation of the references to colour in this figure legend, the reader is referred to the web version of this article.)

The numerical oil spill simulations showed that spills in the easternmost basins of the BEM are more impactful, with oil intrusion exceeding 80 % on the continental shelf and stranding exceeding 30 % along the coastline. In contrast, the oil dispersion simulations from the SFZA basin (Point 4) showed no intrusion or stranding. This result is attributed to a combination of factors, including the considerable width of the continental shelf adjacent, the separation between the 50 m and 100 m isobaths (the first is the criterion of intrusion detection threshold and the latter marking the continental shelf break), and the prevailing wind-driven circulation, which did not favor oil transport toward the coast during the analysis period.

In general, the first three oil release points show that summer and spring have the highest rates of oil intrusion and stranding along the BEM. However, a clear seasonal pattern cannot be determined for the entire region due to the small percentage differences (<10 %) compared to other seasons. An exception to this trend is observed in the SPAMA oil release simulations (point 3), which show significantly higher intrusion and stranding Percentage on the SFZA shelf and coast, respectively, during austral summer. These findings underscore the need for targeted coastal management strategies in the BEM, demanding monitoring and spill response preparedness, and strict regulations for offshore exploration activities. Future research should consider testing additional oil types with distinct viscosities and weathering characteristics, the incorporation of higher-resolution oceans models to solve nearshore dynamics more accurately, and integrating uncertainty quantification methods to improve the robustness of oil spill risk assessments in the region.

## CRediT authorship contribution statement

**Francisco Flávio de Brito Borges:** Writing – review & editing, Writing – original draft, Visualization, Validation, Software, Methodology, Formal analysis, Data curation. **Pedro Paulo de Freitas:** Writing – review & editing, Writing – original draft, Supervision, Resources, Project administration, Methodology, Funding acquisition, Conceptualization. **Wanessa Karoline Lima e Silva:** Writing – review & editing, Visualization, Validation, Software. **Camilo Andrés Guerrero-Martin:** Writing – review & editing. **Vando José Costa Gomes:** Writing – review & editing, Visualization, Supervision. **Eduardo Siegle:** Writing – review & editing, Supervision.

## Funding

Brazilian National Council for Scientific and Technological Development (CNPq) through grant 406506/2022–1. The first author was funded by the Brazilian National Council for Scientific Technological Development (CNPq), grant 406506/2022–1.

## Declaration of competing interest

The authors declare that they have no known competing financial interests or personal relationships that could have appeared to influence

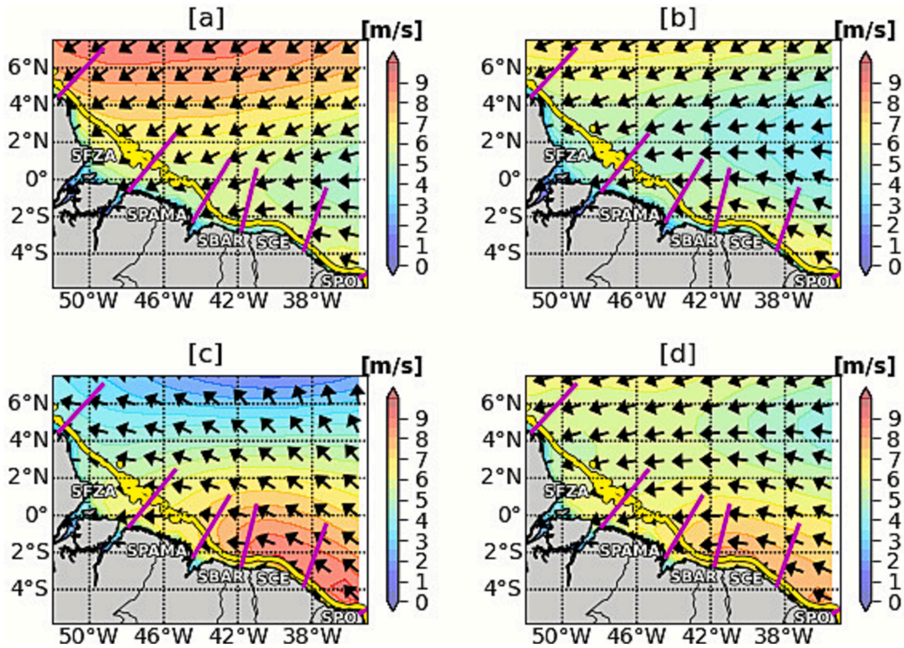


**Fig. 12.** Average wind field from ERA5 along the BEM based on three years (2021–2023) of SMOC model results. Panels [a-d] show the temporal average for the austral summer, autumn, winter, and spring, respectively. The 50 m isobath (yellow line) highlights the approximate mid-shelf region, while the magenta lines indicate the boundaries of the exploratory basins as shown in Fig. 1. (For interpretation of the references to colour in this figure legend, the reader is referred to the web version of this article.)

the work reported in this paper.


## Acknowledgments

The authors thank the Copernicus Marine Service for providing the Surface Merged Ocean Current (SMOC) used in the simulations. We also thank Coriolis platform for the drifter trajectory and velocity data, the AMANDES project and the PNBOIA program for the mooring and buoy data used in the model validation. This research was made possible by funding from the Fundação Amazônia de Amparo a Estudos e Pesquisas (FAPESPA) and the Fundação de Amparo e Desenvolvimento da Pesquisa (FADESP) through grants 015/2019 and 2019/307839. E.S. is a CNPq research fellow. The authors also wish to thank the Brazilian National Council for Scientific and Technological Development (CNPq) for the financial support through grant 406,506/2022–1.


## Data availability

The datasets used and/or generated in this study can be made available by the author upon request.

## References


Abelha, M., 2023. Perspectivas Exploratórias da Margem Equatorial Brasileira. Superintendente de Promoção de Licitações, ANP, apresentação de 14 de junho de 2023. Disponível em: Perspectivas Exploratórias da Margem Equatorial Brasileira — Agência Nacional do Petróleo, Gás Natural e Biocombustíveis. Acesso em: 9 jun.

Abou Samra, R.M., Ali, R., 2022. Monitoring of oil spill in the offshore zone of the Nile Delta using sentinel data. Mar. Pollut. Bull. 179, 113718. https://doi.org/10.1016/j.marpolbul.2022.113718.

Abou Samra, R.M., Ali, R.R., 2024. Tracking the behavior of an accidental oil spill and its impacts on the marine environment in the eastern Mediterranean. Mar. Pollut. Bull. 198, 115887. https://doi.org/10.1016/j.marpolbul.2023.115887.

Abou Samra, R.M., El-Gammal, M., Eissa, R., 2021. Oceanographic factors of oil pollution dispersion offshore the Nile Delta (Egypt) using GIS. Environ. Sci. Pollut. Res. 28, 25830–25843. https://doi.org/10.1007/s11356-021-12570-0.

Aguiar, A.L., Marta-Almeida, M., Cruz, L.O., Pereira, J., Cirano, M., 2022. Forcing mechanisms of the circulation on the Brazilian equatorial shelf. Cont. Shelf Res. 247, 104811. https://doi.org/10.1016/j.csr.2022.104811.

Araújo, J.G., Mello Filho, A. dos S., Peixoto, U.I., Bentes, B., Santos, M.A.S., Dutka-Gianelli, J., Isaac, V., 2022. Multidimensional evaluation of brown shrimp trawling fisheries on the Amazon continental shelf. Front. Mar. Sci. 9, 801758. https://doi.org/10.3389/fmars.2022.801758.

Ávila, R.M., 2022. Are there any analogies between the Foz do Amazonas basin in Brazil and the discoveries in Guyana-Suriname? Apresentação realizada na Superintendência de Avaliação Geológica e Econômica (SAG), ANP, 28 outubro de 2022. Disponível em: Late K-Sandstone Turbidite — Agência Nacional do Petróleo, Gás Natural e Biocombustíveis. Acesso em: 9 jun.

Calzada, A., Delgado, I., Ramos, C., Pérez, F., Reyes, D., Carracedo, D., Rodríguez, A., Chang, D., Cabrales, J., Lobaina, A., 2021. Lagrangian model PETROMAR-3D to describe complex processes in marine oil spills. Open J. Mar. Sci. 11, 17–40. https://doi.org/10.4236/ojms.2021.111002.

da Cruz, C.A., Ribeiro, H.J.S., da Silva, E.B., 2021. Exploratory plays of the Foz do Amazonas Basin, NW portion, in deep and ultra-deep waters, Brazilian equatorial margin. J. S. Am. Earth Sci. 111, 103475. https://doi.org/10.1016/j.jsames.2021.103475.

Dagestad, K.F., Röhrs, J., Breivik, Ø., Ådlandsvik, B., 2018. OpenDrift v1. 0: a generic framework for trajectory modelling. Geosci. Model Dev. 11 (4), 1405–1420. https://doi.org/10.5194/gmd-11-1405-2018.

de Almeida, N.M., Alves, T.M., Nepomuceno Filho, F., Freire, G.S.S., Souza, A.C.B., Oliveira, K.M.L., Barbosa, T.H.S., 2020. A three-dimensional (3D) structural model for an oil-producing basin of the Brazilian equatorial margin. Mar. Pet. Geol. 122, 104599. https://doi.org/10.1016/j.marpetgeo.2020.104599.

de Freitas, P.P., Cirano, M., Teixeira, C.E.P., Marta-Almeida, M., de Brito Borges, F.F., Guerrero-Martin, C.A., Costa Gomes, V.J., 2024. Pathways of surface oceanic water intrusion into the Amazon continental shelf. Ocean Dyn. 74 (4), 321–334. https://doi.org/10.1007/s10236-024-01606-x.

de Freitas, P.P., Cirano, M., Teixeira, C.E.P., Melres, S.J.R., Gomes, V.J.C., Guerrero-Martin, C.A., Koch-Larrouy, A., 2025. Spatial and temporal variability of hydrodynamics on the Amazon continental shelf: an observational approach. Cont. Shelf Res., 105491 https://doi.org/10.1016/j.csr.2025.105491.

Duke, N.C., 2016. Oil spill impacts on mangroves: recommendations for operational planning and action based on global review. Mar. Pollut. Bull. 109 (1), 700–715. https://doi.org/10.1016/j.marpolbul.2016.06.082.

Duke, N.C., Pinzon, Z.S., Prada, M.C., 1997. Large-scale damage to mangrove forests following two large oil spills in Panama. Biotropica 29, 2–14.

French-McCay, D.P., 2004. Oil spill impact modeling: development and validation. Environ. Toxicol. Chem. 23 (10), 2441–2456. https://doi.org/10.1897/03-382.

Galieriková, A., Materna, M., 2020. World seaborne trade with oil: one of main cause for oil spills? Transportation research procedia 44, 297–304. https://doi.org/10.1016/j.trpro.2020.02.039.

Goes, E.R., Mallmann, D.L.B., Brown, C.J., Maida, M., Ferreira, B.P., de Araújo, T.C.M., 2023. A seafloor sensitivity index to oil spills in tropical marine protected areas. Cont. Shelf Res. 266, 105069. https://doi.org/10.1016/j.csr.2023.105069.

Govindarajan, S.K., Mishra, A., Kumar, A., 2021. Oil spill in a marine environment: requirements following an offshore oil spill. Rudarsko-geološko-naftni zbornik 36 (4). https://doi.org/10.17794/rgn.2021.4.1.

Hayworth, J.S., Clement, T.P., Valentine, J.F., 2011. Deepwater horizon oil spill impacts on Alabama beaches. Hydrol. Earth Syst. Sci. 15, 3639–3649. https://doi.org/10.5194/hess-15-3639-2011.

Hoorn, C., Bogotá-A, G.R., Romero-Baez, M., Lammertsma, E.I., Flantua, S.G., Dantas, E. L., Chemale Jr., F., 2017. The Amazon at sea: onset and stages of the Amazon River from a marine record, with special reference to Neogene plant turnover in the drainage basin. Glob. Planet. Chang. 153, 51–65. https://doi.org/10.1016/j.gloplacha.2017.02.005.

Huettel, M., 2022. Oil pollution of beaches. Curr. Opin. Chem. Eng. 36, 100803. https://doi.org/10.1016/j.coche.2022.100803.

Landim Dominguez, J.M., Papa de Kikuchi, R.K., de Araujo Filho, M.C., Schwamborn, R., Vital, H. (Eds.), 2023. Tropical Marine Environments of Brazil. Spatio-temporal Heterogeneities and Responses to Climate Changes, xvi. Springer, Cham, p. 266. https://doi.org/10.1007/978-3-031-21329-8. ISBN 978–3–031–21328-1; e-ISBN 978–3–031–21329-8.

Lavagnino, A.C., Bastos, A.C., Amado Filho, G.M., De Moraes, F.C., Araujo, L.S., de Moura, R.L., 2020. Geomorphometric seabed classification and potential megahabitat distribution in the Amazon continental margin. Front. Mar. Sci. 7, 190. https://doi.org/10.3389/fmars.2020.00190.

Le Bars, Y., Lyard, F., Jeandel, C., Dardengo, L., 2010. The AMANDES tidal model for the Amazon estuary and shelf. Ocean Model 31 (3–4), 132–149. https://doi.org/10.1016/j.ocemod.2009.11.001.

Le Tan, C., Van, P.N., Hong, Q.N., Diem, L.T.T., Thanh, M.T., 2023. A framework for assessing environmental incidents in coastal areas: a case study in the southeastern coastal area of Vietnam. Appl. Environ. Res. 45 (1). https://doi.org/10.35762/AER.2023002.

Lessa, G.C., Teixeira, C.E.P., Pereira, J., Santos, F.M., 2021. The 2019 Brazilian oil spill: insights on the physics behind the drift. J. Mar. Syst. 222, 103586. https://doi.org/10.1016/j.jmarsys.2021.103586.

Lewis, M., Pryor, R., Wilking, L., 2011. Fate and effects of anthropogenic chemicals in mangrove ecosystems: A review. Environ. Pollut. 159 (10), 2328–2346. https://doi.org/10.1016/j.envpol.2011.04.027.

Louchard, D., Gruber, N., Münnich, M., 2021. The impact of the Amazon on the biological pump and the air-sea $CO_2$ balance of the Western tropical Atlantic. Glob. Biogeochem. Cycles 35, e2020GB006818. https://doi.org/10.1029/2020GB006818.

Mahiques, M.M., Siegle, E., Francini-Filho, R.B., Thompson, F.L., Rezende, C.E., Gomes, J.D., Asp, N.E., 2019. Insights on the evolution of the living great Amazon reef system, equatorial West Atlantic. Sci. Rep. 9, 13699. https://doi.org/10.1038/s41598-019-50245-6.

Mello, M.R., Takaki, T., Fontes, C.A., Mohriak, W., Barbanti, S.M., Azambuja Filho, N.C., Bender, A.A., 2013, October. New deep water frontiers in the South Atlantic equatorial margins. In: Offshore Technology Conference Brasil. OTC, pp. OTC–24361. https://doi.org/10.4043/24361-MS.

Milani, E.J., Brandão, J.A.S.L., Zalán, P.V., Gamboa, L.A.P., 2000. Petróleo na margem continental brasileira: geologia, exploração, resultados e perspectivas. Rev Bras Geofis 18, 352–396. https://doi.org/10.1590/S0102-261X2000000300012.

Moura, R.L., Amado-Filho, G.M., Moraes, F.C., Brasileiro, P.S., Salomon, P.S., Mahiques, M.M., Bastos, A.C., Almeida, M.G., Silva, J.M., Araújo, B.F., Brito, F.P., Rangel, T.P., Oliveira, B.C.V., Bahia, R.G., Paranhos, R.P., Dias, R.J.S., Siegle, E., Figueiredo, A.G., Pereira, R.C., Leal, C.V., Hajdu, E., Asp, N.E., Gregoracci, G.B., Neumann-Leitão, S., Yager, P.L., Francini-Filho, R.B., Froes, A., Campeão, M., Silva, B.S., Moreira, A.P.B., Oliveira, L., Soares, A.C., Araújo, L., Oliveira, N.L., Teixeira, J.B., Valle, R.A.B., Thompson, C.C., Rezende, C.E., Thompson, F.L., 2016. An extensive reef system at the Amazon River mouth. Sci. Adv. 2, e1501252. https://doi.org/10.1126/sciadv.1501252.

Nguyen, T.H.H., Hou, T.H., Pham, H.A., Tsai, C.C., 2024. Oil spill sensitivity analysis of the coastal waters of Taiwan using an integrated modelling approach. J Mar Sci Eng 12 (1), 155. https://doi.org/10.3390/jmse12010155.

Nittrouer, C.A., DeMaster, D.J., 1986. Sedimentary processes on the Amazon continental shelf: past, present and future research. Cont. Shelf Res. 6 (1–2), 5–30. https://doi.org/10.1016/0278-4343(86)90051-8.

Nittrouer, C.A., DeMaster, D.J., 1996. The Amazon shelf setting: tropical, energetic, and influenced by a large river. Cont. Shelf Res. 16, 553–573. https://doi.org/10.1016/0278-4343(95)00069-0.

Nobre, P., Lemos, A.T., Giarolla, E., Camayo, R., Namikawa, L., Kampel, M., Polito, P.S., 2022. The 2019 Northeast Brazil oil spill: scenarios. An. Acad. Bras. Cienc. 94 (Suppl. 2), e20210391. https://doi.org/10.1590/0001-3765202220210391.

Nunes, B.Z., Soares, M.O., Zanardi-Lamardo, E., Castro, I.B., 2023. Marine protected areas affected by the most extensive oil spill on the southwestern Atlantic coast. Ocean Coast. Res. 71 (2), e23028. https://doi.org/10.1590/2675-2824071.22153bzn.

Ozorio, C.P., Guiloski, I.C., de Assis, H.C.S., Martins, C.C., Sandrini-Neto, L., Lana, P.C., 2024. Oxidative stress and neurotoxicity in *Scolelepis goodbodyi* (Polychaeta, Spionidae) after an experimental oil spill in a dissipative sandy beach. Ocean and Coastal Research 72 (1), e24012. https://doi.org/10.1590/2675-2824072.23116.

Pabón, R.E.C., de Souza Filho, C.R., 2019. Crude oil spectral signatures and empirical models to derive API gravity. Fuel 237, 1119–1131. https://doi.org/10.1016/j.fuel.2018.09.098.

Pavlov, V., James, N.A., Masden, E.A., de Aguiar, V.C.M., Hole, L.R., Liimatainen, H., Pongrácz, E., 2023. Impacts of offshore oil spill accidents on island bird communities: A test run study around Orkney and Svalbard archipelagos. Environ. Pollut. 334, 122193. https://doi.org/10.1016/j.envpol.2023.122193.

Pena, P.G.L., Northcross, A.L., Lima, M.A.G.D., Rêgo, R.D.C.F., 2020. Derramamento de óleo bruto na costa brasileira em 2019: emergência em saúde pública em questão. Cad. Saude Publica. 36, e00231019. https://doi.org/10.1590/0102-311X00231019.

Peterson, C.H., Rice, S.D., Short, J.W., Esler, D., Bodkin, J.L., Ballachey, B.E., Irons, D.B., 2003. Long-term ecosystem response to the Exxon Valdez oil spill. Science 302 (5653), 2082–2086. https://doi.org/10.1126/science.1084282.

Prestes, Y.O., da Silva, A.C., Jeandel, C., 2018. Amazon water lenses and the influence of the North Brazil current on the continental shelf. Cont. Shelf Res. 160, 36–48. https://doi.org/10.1016/j.csr.2018.04.002.

Price, L., Mapes, R., 2023. Frontier exploration on the equatorial margin: How Guyana geoscience can frame success strategies. In: First EAGE Conference on Deepwater Equatorial Margin: New Energy Frontier for South America, 2023. European Association of Geoscientists & Engineers, pp. 1–4. https://doi.org/10.3997/2214-4609.202380030. No. 1.

Reed, M., Johansen, Ø., Brandvik, P.J., Daling, P., Lewis, A., Fiocco, R., Mackay, D., 1999. Oil spill modeling towards the close of the 20th century: overview of the state of the art. Spill Sci Technol Bull 5 (1), 3–16. https://doi.org/10.1016/S1353-2561(98)00029-2.

Santos, L.C.M., Cunha-Lignon, M., Schaeffer-Novelli, Y., Cintrón-Molero, G., 2012. Long-term effects of oil pollution in mangrove forests (Baixada Santista, Southeast Brazil) detected using a GIS-based multitemporal analysis of aerial photographs. Braz. J. Oceanogr. 60 (2), 159–170.

Soares, M.O., Teixeira, C.E.P., Bezerra, L.E.A., et al., 2022. The most extensive oil spill registered in tropical oceans (Brazil): the balance sheet of a disaster. Environ. Sci. Pollut. Res. 29, 19869–19877. https://doi.org/10.1007/s11356-022-18710-4.

Transportation Research Board and National Research Council, 2003. Oil in the Sea III: Inputs, Fates, and Effects. The National Academies Press, Washington, DC. https://doi.org/10.17226/10388.

Uno, S., Kokushi, E., Añasco, N.C., Iwai, T., Ito, K., Koyama, J., 2017. Oil spill off the coast of Guimaras Island, Philippines: distributions and changes of polycyclic aromatic hydrocarbons in shellfish. Mar. Pollut. Bull. 124 (2), 962–973. https://doi.org/10.1016/j.marpolbul.2017.03.062.

Ysaccis, R., Earney, M., Alvarez, F., Moreira, L., Silenziario, C., 2023, June. New insights into the hydrocarbon potential of Brazil's equatorial basins: An underexplored Atlantic margin. In: 84th EAGE Annual Conference & Exhibition, 2023. European Association of Geoscientists & Engineers, pp. 1–5. https://doi.org/10.3997/2214-4609.202310115. No. 1.

Zacharias, D.C., Lemos, A.T., Keramea, P., Dantas, R.C., da Rocha, R.P., Crespo, N.M., Lourenço, R.A., 2024. Offshore oil spills in Brazil: an extensive review and further development. Mar. Pollut. Bull. 205, 116663. https://doi.org/10.1016/j.marpolbul.2024.116663.